

RICE UNIVERSITY

**Directional Antenna Diversity for Mobile Devices:
Characterizations and Solutions**

by

Ardalan Amiri Sani


A THESIS SUBMITTED
IN PARTIAL FULFILLMENT OF THE
REQUIREMENTS FOR THE DEGREE

Master of Science

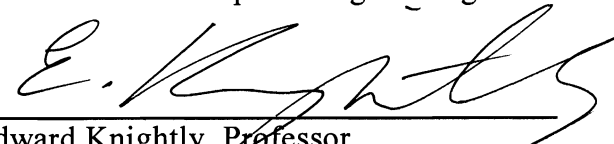
APPROVED, THESIS COMMITTEE:



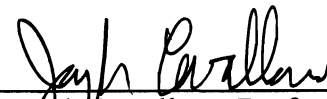
Lin Zhong, Chair, Assistant Professor
Electrical and Computer Engineering



Ashutosh Saharwal, Associate Professor
Electrical and Computer Engineering



Edward Knightly, Professor
Electrical and Computer Engineering



Joseph Cavallaro, Professor
Electrical and Computer Engineering

HOUSTON, TEXAS
APRIL 2011

ABSTRACT

Directional Antenna Diversity for Mobile Devices: Characterizations and Solutions

by

Ardalan Amiri Sani

We report a first-of-its-kind realization of directional transmission for smartphone-like mobile devices using multiple passive directional antennas, supported by only one RF chain. The key is a multi-antenna system (MiDAS) and its antenna selection methods that judiciously select the right antenna for transmission. It is grounded by two measurement-driven studies regarding 1) how smartphones rotate during wireless usage in the field and 2) how orientation and rotation impact the performance of directional antennas under various propagation environments.

We implement MiDAS using the WARP platform, and evaluate it using a computerized motor to rotate the prototype according to traces collected from smartphone users in the field. Our evaluation shows MiDAS achieves median of 3dB increase in link gain. Combined with rate adaptation and power control, MiDAS also improves goodput and power saving. MiDAS does not require any changes to the network infrastructure, and is therefore suitable for immediate deployment.

Acknowledgements

I am thankful to my advisor, Professor Lin Zhong, for his encouragement, guidance, and support, which helped me to develop a better understanding of scientific research. I am also thankful to Professor Ashutosh Sabharwal who advised me on my thesis work too. Without his help, this thesis would not be in its current shape.

I would like to thank Professor Edward Knightly and Professor Joseph Cavallaro for serving on the thesis committee. Their comments and feedback to this work have been of great value.

I would like to thank former group member and friend, Hasan Dumanli, who started the directional antenna work in the group. I owe him for passing to me his expertise.

I am grateful to my family and my friends, who have always been a great support for me.

Lastly, I thank all of those who helped me towards the completion of this thesis.

Contents

ABSTRACT.....	ii
Acknowledgements.....	iii
Contents	iv
List of Figures	vii
List of Tables.....	ix
Chapter 1 Introduction.....	1
Chapter 2 Directional Antennas.....	5
Chapter 3 Characterizing Smartphone Rotation	7
3.1 Smartphone Orientation Estimation	7
3.2 Rotation Speed.....	9
3.3 Predictability of Orientation.....	10
Chapter 4 Characterizing Directional Propagation	11
4.1 Experimental Setup.....	11
4.2 Impact of Orientation.....	13
4.3 Channel Reciprocity	14
4.4 Superiority of Directional Antennas.....	15
4.5 Predictability of RSS	17
Chapter 5 Multi-Antenna Design (MiDAS)	18

Chapter 6	Selection for Legacy Networks	20
6.1	Packet-based Antenna Assessment.....	20
6.2	Antenna Bookkeeping	21
6.3	Heuristic Antenna Selection Algorithm	22
Chapter 7	Selection with PHY Support	25
7.1	PHY Symbol-based Antenna Assessment.....	25
7.2	Selection Feedback	26
Chapter 8	Evaluation.....	28
8.1	Hardware Implementation	28
8.2	Trace Collection	29
8.3	Trace-based Simulation	30
8.4	Number of Directional Antennas:.....	33
8.5	Moving Scenario.....	35
Chapter 9	MiDAS with Rate Adaptation and Power Control.....	36
9.1	Simulation Results.....	37
9.2	Real-Time Experiment Results.....	39
Chapter 10	MiDAS with Rate Adaptation and Power Control	42
Chapter 11	Conclusions	44
References	46

Appendix A Trace Collection	50
Appendix B Euler Angle Estimation	51
B.1. Deriving Euler Angles.....	51
B.2. Overcoming Hardware Limitation	52
B.3. Validation of Orientation Estimation	53

List of Figures

Figure 1: Euler angles in the ZYX convention used in our characterization of smartphone orientation and rotation	8
Figure 2: Cumulative Distribution Function (CDF) of rotation speed for three Euler angles, calculated for 0.1s, 1s, and 10s intervals	9
Figure 3: Error($^{\circ}$) of orientation prediction from 10ms to 10s	9
Figure 4: Rotation platform for directional channel characterization. The motor can replay field-collected traces or orient the WARP board toward any given direction in the azimuth plane	12
Figure 5: Directional antenna patterns in NLOS and LOS indoor environments.....	13
Figure 6: Distribution of superiority intervals in terms of the percentage of the total replay time in NLOS indoor	16
Figure 7: RSS prediction error for the 5dBi and 8dBi directional antennas for 10ms to 10s intervals.....	16
Figure 8: Multi-antenna system with one omni directional antenna and one or more directional antennas that works with existing wireless interfaces with a single transceiver	19
Figure 9: The packet-based antenna selection with two modes: Best and Safe. The client transits between the two modes according to two decisions.....	23
Figure 10: Two different ways for the receiver to notify the mobile client of the best antenna for symbol-based antenna selection.....	26

Figure 11: (a) Physical arrangement of the three directional antennas used in the trace collection and experimentation (b) A segment of RSSI trace for three 5dBi antennas in NLOS indoor environment	29
Figure 12: Impact of system settings on the performance of the multi-antenna system. Each bar presents the median, 10 th and 90 th percentile gain for three antenna selection cases: 1) <i>upper bound</i> assuming the best antenna is always used; 2) <i>symbol-based</i> antenna selection described in Chapter 7; and 3) <i>packet-based</i> antenna selection described in Chapter 6	32
Figure 13: Impact of number of directional antennas on the performance of <i>upper bound</i> , MiDAS <i>symbol-based</i> , and MiDAS <i>packet-based</i>	34
Figure 14: (a) Goodput of MiDAS+RA/PC (three 5dBi and three 8dBi) and Omni+RA in NLOS indoor; (b) Goodput Gain (GG) and transmit Power Reduction (PR) of MiDAS+RA/PC (three 5dBi) versus omni+RA in NLOS indoor	38
Figure 15: Effective goodput of different modulations in WARP with equal-air-time packets.....	40

List of Tables

Table 1: Orientation estimation error (°)	54
---	----

Chapter 1 Introduction

Current mobile devices, such as smartphones and laptops, are omni directional and radiate power to all directions for uplink transmission. Omni directionality not only introduces interference between peers, but also leads to power waste. Emerging smartphone applications, such as participatory sensing, media sharing, mobile health monitoring, and video chat, are increasingly employing the uplink. Therefore, the mentioned interference has become a key bottleneck in the capacity of infrastructure networks with a large number of mobile clients. Similarly, the power waste also makes wireless transmission one of the most power-hungry activities on mobile devices, contributing a critical barrier to the usability and wider adoption of mobile Internet. Furthermore, devices that are far away from access points or base stations, also suffer from low uplink data rates since most of their limited transmission power is radiated to undesirable directions.

Directional transmission can alleviate these problems by focusing the radiation toward the intended receiver. Beamforming employs multiple RF chains to achieve directionality. However, its cost and power overhead has prevented it from being immediately used on smartphone-like mobile devices. In this work, we study a much more efficient way of realizing directionality: *miniature passive directional antennas*. Many authors use “directional antenna” to refer to beamforming based on smart antennas. In this work, we use “antenna” to refer to the passive antenna without the RF chain. By placing multiple directional antennas on the surface of a mobile device, the device can opportunistically select one for directional transmission without adding RF circuitry, in contrast to the

simultaneous use of multiple RF chains by beamforming. However, because only one antenna can be used at a time, the device will not be able to find out the best antenna easily, especially when it moves and rotates.

The goal of this work is to realize the benefits of directional antennas for mobile devices. Toward this goal, we experimentally answer three questions.

First, how do smartphone-like mobile device rotate during wireless access? By using a directional antenna, the device orientation becomes critical because a mobile device can rotate and the rotation changes device direction much faster than mobility does. We collect accelerometer and compass readings along with network usage information from 11 smartphone users, each for one week in the field. From such field-collected traces, we are able to estimate the orientation and rotation of the smartphones during wireless usage. We show that smartphones rotate relatively slowly; compared to how fast packets are exchanged during wireless communication. Moreover, the orientation is quite predictable in short intervals. We report the characterization in Chapter 3.

Second, how do directional antennas behave with indoor and non-line-of-sight (NLOS) propagations? While recent work has shown directional communication can work well with stationary nodes for indoor and NLOS propagation [1, 2], it is still unclear how orientation and rotation would impact the directional channels. Therefore, using a computerized motor platform, we measure the Received Signal Strength Indicator (RSSI) of directional antennas for indoor and NLOS environments, with not only controlled orientations, but also rotation according to the field-collected traces. We show that directional antennas outperform omni ones for a considerable range of orientations even in NLOS indoor environments. More importantly, the directional channels are

highly reciprocal for 802.11-like frequency bands, and their performance is quite predictable in short intervals even under realistic rotations. We report the characterization in Chapter 4.

Finally, how can a device dynamically select the best antenna? Leveraging the discoveries from the two characterizations, we design a multi-antenna system (MiDAS) that consists of an omni directional antenna, one or more directional antennas, and an antenna switch. MiDAS works with existing mobile devices that usually have a single RF chain and can use only one antenna at a time. We further provide two antenna selection methods for MiDAS. The packet-based method uses one packet to assess an antenna without any changes to the network infrastructure. The symbol-based method uses the PHY training symbols so that all antennas are assessed with a single packet. It is much more efficient than the packet-based selection but requires changes to the PHY layer. We report the design of MiDAS in Chapter 5 and the two antenna selection methods in Chapter 6 and Chapter 7, respectively.

We implement MiDAS and its antenna selection methods on the WARP platform from Rice University and evaluate them with the computerized motor platform that replays the field-collected rotation traces from smartphone users. Our evaluation shows that with three 5dBi directional antennas placed on the surfaces of a device, MiDAS can achieve a median gain close to 3dB, without any changes to the network infrastructure.

To fully realize the benefits of the link gain of MiDAS, we incorporate rate adaptation and power control mechanisms into our system. Using real-time experiments, we demonstrate that MiDAS can improve the link goodput by 85% when the SNR is low.

Also, when the SNR is high, it can save 51% of the transmit power, while increasing the goodput by 7%. We report the prototype and evaluation in Chapter 8.

To the best of our knowledge, this work represents the first publicly available characterizations of the rotation of smartphone-like devices and its impact on the performance of directional antennas. MiDAS and its antenna selection methods are also the first reported directionality implementation for a device that cannot only move but can also rotate. We will discuss related work in Chapter 9.

Making smartphone-like devices directional is a radical departure from existing and emerging wireless technologies. It provides an inexpensive and immediately deployable solution to improve network capacity and device efficiency. While we demonstrate the effectiveness of MiDAS in improving link goodput and device power efficiency, more network support is needed to fully realize its potential in improving network capacity. From this perspective, our work complements existing work on directional MAC protocol design, e.g., [3].

This thesis work was included in a conference paper at MobiCom 2010 [4].

Chapter 2 Directional Antennas

We are motivated by the commercial availability of miniature passive directional antennas that can be employed on mobile devices. Microstrip antennas are good examples. The microstrip antennas used in our prototype have a patch area of 3.2×3.2 cm² [5]. This allows the placement of these antennas on front and back sides of smartphones. Also theoretically, the width of the patch can be even smaller while maintaining 5dBi or 8dBi peak gain. This will enable thin directional microstrip antennas to be placed on other sides of smartphones.

Moreover, recent advances in multiple reconfigurable antennas have produced small form factor antennas with a few directional beams in different directions [6, 7]. Also, sectorized antennas [8] are another option for having multiple beams on a mobile device. But, due to their larger size, they can be used for bigger mobile devices, such as iPad, Kindle, or netbooks.

Unlike digital beamforming, the passive directional antennas discussed above produce a directional radiation pattern without extra circuitry or power. With a directional radiation pattern pointed at the right direction, a mobile client can use reduced transmit power to deliver a required receiver signal strength (RSS), or it can increase the RSS with the same transmit power. In both cases, the client's interference to its peers is reduced.

The key challenge to the use of directional antennas on mobile devices is that a mobile device can change its orientation through mobility and rotation. Since one directional antenna can only provide adequate gain for a limited range of orientations, multiple

antennas should be placed around the device so that they collectively provide a much larger range of orientations in which at least one of them provides adequate gain.

Because directional antennas have never been studied for smartphone-like mobile devices before, the key questions regarding their feasibility naturally arises:

Is it possible to track the right antenna when a mobile device can not only move but can also rotate?

We next answer this question experimentally in three steps.

Chapter 3 Characterizing Smartphone Rotation

We first characterize the orientation and rotation of smartphones during wireless access with data collected from field usage. It is important to note that the relative direction of a device with its access point (base station) is determined by not only device orientation but also location. We do not include location in our characterization because mobile client location and its changes have been extensively studied as mobility. Moreover, change in relative direction due to mobility is much slower than that due to rotation thanks to the large distance between a mobile device and its access point or base station.

3.1 Smartphone Orientation Estimation

We have collected accelerometer and compass readings from 11 smartphone users, each for one week along with both voice and data usage. The average usage time for a participant is 25.9 hours. See Appendix A for the trace collection details. The traces will also be used in the characterization and evaluation reported later in this submission. The collected data are available through CRAWDAD [9].

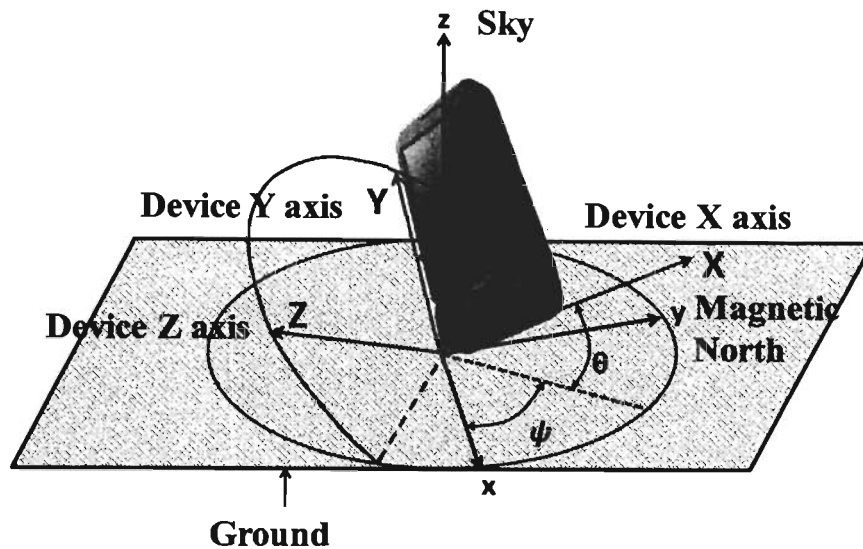


Figure 1: Euler angles in the ZYX convention used in our characterization of smartphone orientation and rotation

We are able to derive the smartphone orientation, represented by three *Euler angles* [10] under the ZYX convention. According to Euler Theorem, the orientation of a rigid body can be uniquely defined by three angles, also known as Euler angles. These three Euler angles are shown as θ , φ , and ψ in Figure 1. The X, Y and Z axes are the coordinates of the device, meaning that they are fixed to the body of the device and rotate with it. The x, y and z axes (lower case) represent the axes of the earth. The z axis points to the sky and is perpendicular to the ground. The y axis is parallel to the ground and points to the magnetic north. The x axis is also parallel to the ground and is orthogonal to z and y.

Calculating the three Euler angles using a tri-axis accelerometer and a tri-axis compass is straightforward in theory. Because the accelerometer is less subject to external interference, we use the accelerometer and the gravity to derive two of the angles, θ and φ , similar to [11]; we only use the compass for ψ , which is impossible to calculate with the

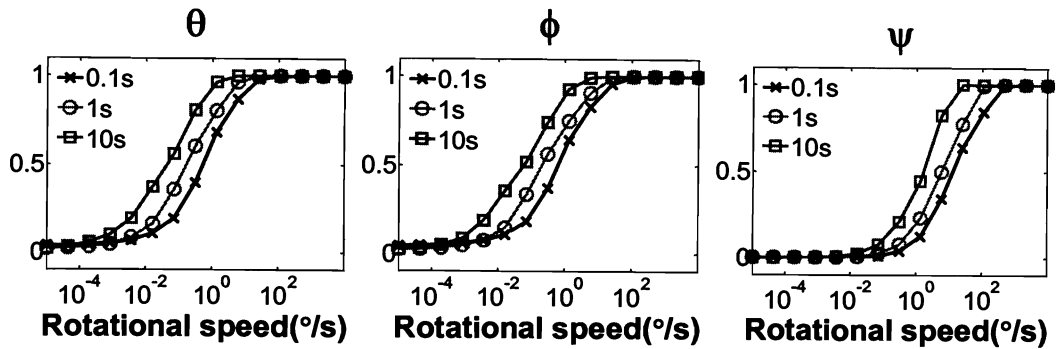


Figure 2: Cumulative Distribution Function (CDF) of rotation speed for three Euler angles, calculated for 0.1s, 1s, and 10s intervals

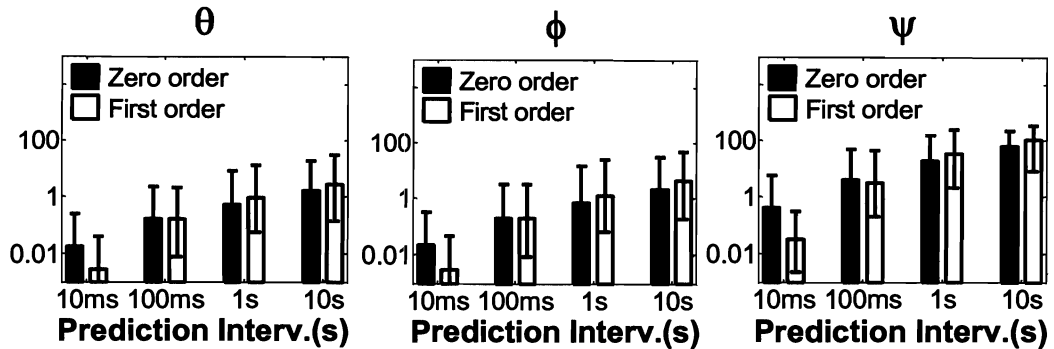


Figure 3: Error($^{\circ}$) of orientation prediction from 10ms to 10s

accelerometer only. In Appendix B, we provide our method for estimating the orientation, and we provide the details regarding how we overcome the practical challenges in orientation estimation.

3.2 Rotation Speed

We next examine how a smartphone changes its orientation, or rotates, when wireless is used. We compute the rotation speed as a vector including three elements, the rates of change of the Euler angles: θ , ϕ , and ψ . We calculate the rotation speed for each of the Euler angles for different time intervals, 0.1s, 1s, and 10s, for the collected traces. Figure 2 shows the distributions of the rotation speed for each Euler angle. We also find that

rotation speeds are below 120 °/second for 90% of time. Such low rotation speeds indicate that the use of directional antennas can be feasible because they outperform the omni directional antenna by several tens of degrees, as we will show in Chapter 4.

Furthermore, the figures show that the rotation distributions are not the same for the three Euler angles. ψ , the angle around the z axis, experiences much faster rotation than the other two angles. Therefore, we will focus on the impact of rotation in ψ in the next few chapters.

3.3 Predictability of Orientation

We examine how accurate one can predict the device orientation in the future, given the past orientations. Let s_n denotes the n th sample of the orientation, measured at time t_n . Prediction is to determine s_{n+1} at t_{n+1} , given t_i and s_i for $i \leq n$. We study two very simple prediction methods.

- Zero order prediction: $s_{n+1} = s_n$, and
- First order prediction: $s_{n+1} = s_n + (s_n - s_{n-1})(t_{n+1} - t_n)/(t_n - t_{n-1})$, which predicts using linear extrapolation.

We evaluate both of the methods on the three Euler angles in predicting for 10ms, 100ms, 1s, and 10s ahead, respectively. Figure 3 summarizes the results. It shows that for predictions of 10ms and 100ms, median errors are below 0.2°, 0.2°, and 3.0° for θ , ϕ , and ψ , respectively. This demonstrates that a phone orientation is quite predictable in short terms, thanks to the continuous nature of human movement.

Chapter 4 Characterizing Directional Propagation

In this chapter, we report experimental characterization of the quality of directional links under various propagation environments, orientation, and rotation. While a few recent works have reported NLOS indoor performance of directional links [1, 2], no one has characterized NLOS indoor directional propagation under device rotation.

4.1 Experimental Setup

We employ two WARP nodes for our experiments. Like most commercial wireless interfaces, the RSSI of the WARP radio card can be read from software. The RSSI values are then translated to RSS values according to the datasheet [12]. We report our results in RSS format in dBm. Considering that the noise floor is approximately constant over time in our hardware, RSS and SNR will just be an additive constant different. Therefore, all RSS results can be easily translated to SNR. Also, maximizing received RSS is equivalent to maximizing received SNR.

We developed a computerized motor platform to rotate one WARP node and its companion laptop in order to emulate the orientation and rotation of a mobile client around the z axis, or ψ . As characterized in Chapter 3, ψ sees the most rotation among the three Euler angles. Also, because we mount the directional antennas perpendicular to the z axis, rotation around the z axis is the most challenging in terms of directional channel changes, as illustrated by Figure 4. Therefore, we believe the evaluation with the motor platform will reveal key insights into the feasibility of directional antennas.

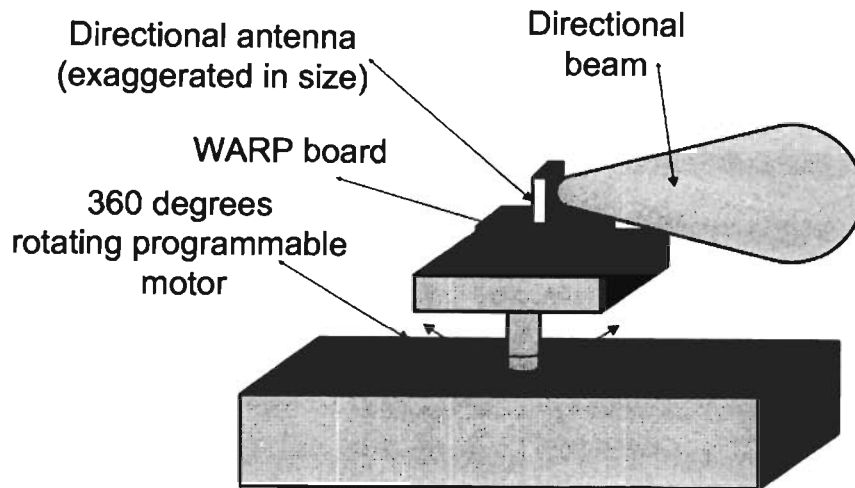


Figure 4: Rotation platform for directional channel characterization. The motor can replay field-collected traces or orient the WARP board toward any given direction in the azimuth plane

Two directional antennas of 5dBi [5] and 8dBi [13] with 85° and 75° half-power horizontal beamwidth respectively, and a close-to-omni directional antenna [14] are used and characterized on this motor-driven WARP node.

A second WARP node with an omni directional antenna is used as the access point (AP). During the experiments, the motor-driven client transmits 802.11-like packets to the AP continuously and as fast as possible. The AP node records the RSSI for every data packet, and the motor-driven node records the RSSI for every ACK packet sent back from the AP.

All indoor experiments are carried out on the third floor of Duncan Hall, an office building at Rice University. Outdoor experiments are carried out in an open space outside Duncan Hall. During the experiments, the client and AP nodes are separated as allowed by the WARP nodes, ~15 meters in most cases. For indoor, experiments are carried out at

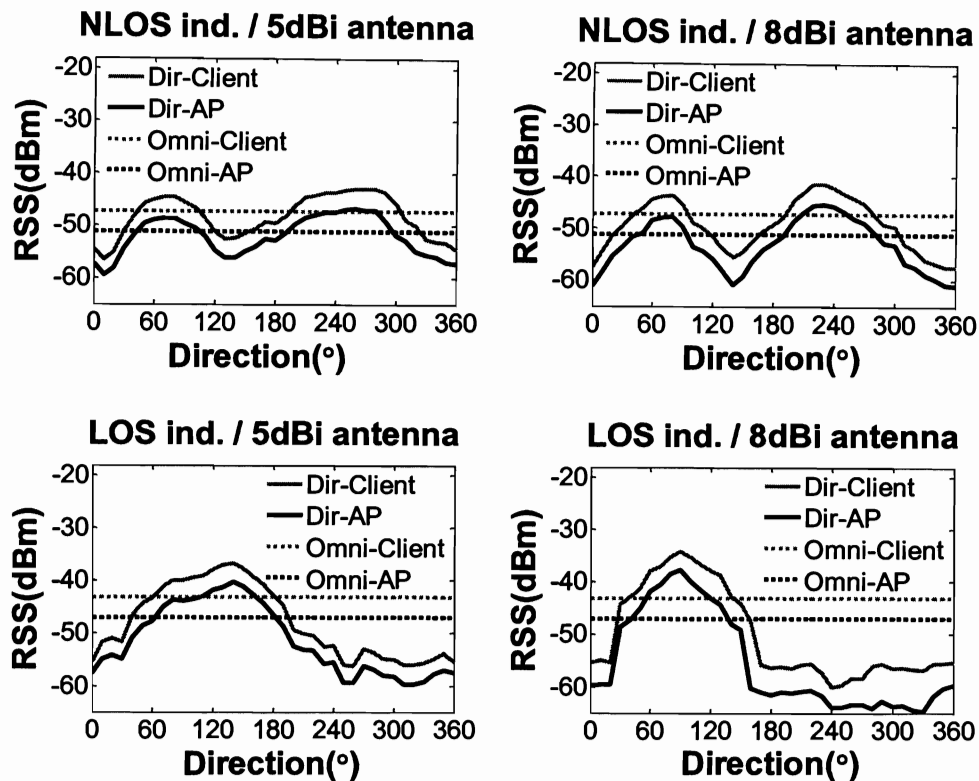


Figure 5: Directional antenna patterns in NLOS and LOS indoor environments

various locations in the building with and without light-of-sight propagation paths, or *LOS indoor* and *NLOS indoor*. The distance between the AP and client in our indoor experiments is comparable to such distance in an enterprise 802.11 network. Indoor environments have been known to be much more challenging for directional communication than outdoor LOS propagation.

4.2 Impact of Orientation

By orienting the motor-driven node toward different directions, we measure the RSSI of directional antennas every 10° in a full circle (360°). We repeat the same experiment in LOS and NLOS indoor environments at various locations. Figure 5 presents traces of

the RSSI measured at the AP for the omni-directional, 5dBi and 8dBi directional antennas at two representative locations. We make the following observations.

First, the RSSI pattern of a directional antenna may significantly deviate from the antenna gain pattern. This is especially true in NLOS environments. Such deviation is largely due to the rich multipath effects.

Second, the RSSI pattern is largely continuous. With the continuity in device rotation and orientation predictability, such RSSI continuity is likely to lead to high predictability in RSSI in real usage, as will be seen in Chapter 4.5.

Third, the directional antenna outperforms the omni directional one over a considerable range of orientation but is significantly worse over some other range. This highlights the potential benefit and risk of using a directional antenna.

Finally, the gain of the directional antenna impacts such benefit and risk. The higher the gain (8dBi vs. 5dBi), the higher the benefit, and the higher the risk. Higher gain antennas have higher peak gains (benefit), but they have deeper valleys and smaller ranges in which the directional antenna is better (risk), as can be seen in Figure 5. In Chapter 8, we will show how such effects affect the performance of MiDAS.

4.3 Channel Reciprocity

By comparing the RSSI of a data packet at the AP against the RSSI of the packet's ACK at the motor-driven client, we examine how reciprocal the channel is for directional antennas. Figure 5 presents both the data packet RSSI and that of its ACK for both the directional and the omni directional antenna. While there is an almost constant gap between the RSSI at the mobile client and that at the AP due to their hardware

personalities, their RSSI track each other closely in their changes. This suggests that *the channel for a directional antenna can be considered reciprocal*. Note that the constant gap between these two measurements is mainly due to different radio characteristics. In Chapter 6, we will leverage this to design a packet-based antenna selection method that selects the antenna for transmission based on RSSI of received packets. It is worth noting that the reciprocity of 802.11 channels of omni directional antennas has been shown by others, e.g., [15].

4.4 Superiority of Directional Antennas

An important question about the use of directional antennas on a mobile device is how long a directional antenna can remain better than the omni one. To answer this question, we randomly select ~6 minutes of rotation traces from each of the 11 participants (one hour in total), and replay them on the computerized motor platform by changing ψ accordingly. During the replay, the mobile client sends packets continuously. In each packet, one directional antenna and one omni antenna take turn and transmit 128 training symbols each. The AP records the RSSI measured for all packets.

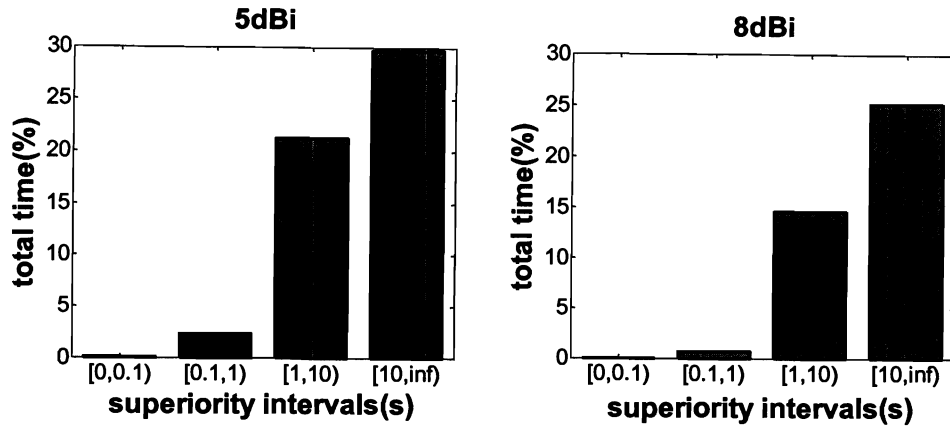


Figure 6: Distribution of superiority intervals in terms of the percentage of the total replay time in NLOS indoor

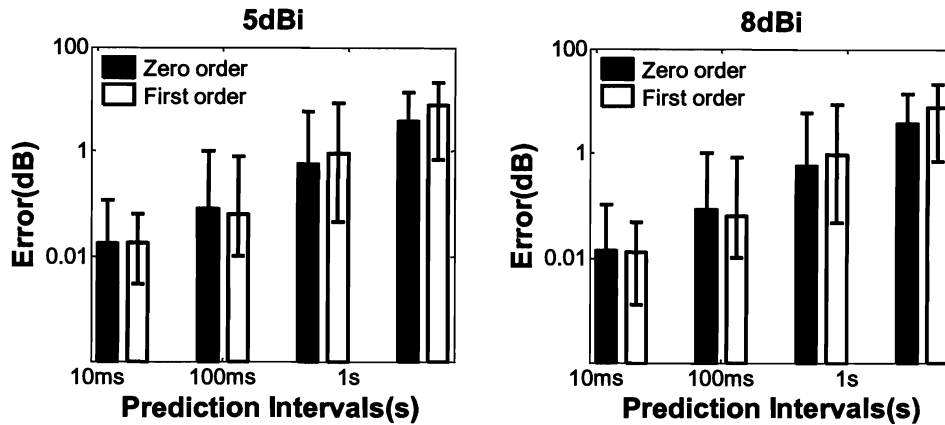


Figure 7: RSS prediction error for the 5dBi and 8dBi directional antennas for 10ms to 10s intervals

By analyzing the entire RSSI traces, we can calculate the time intervals in which the directional antenna is always better than the omni directional one. We call these intervals the *superiority intervals* of the directional antenna. We can also calculate the average RSS gain over the omni directional antennas during such intervals. Figure 6 shows the distribution of superiority intervals in terms of the percentage of the total replay time. It shows that in a NLOS indoor environment, 53% and 40% of the replay time is spent in the superiority intervals over 1s for the 5dBi and 8dBi antenna, respectively. That is,

should the directional antenna be selected, it can provide a better performance over than one second for close to half of the time. The average gain over the omni directional antenna of these superiority intervals is 2.8dB and 2.5dB for 5dBi and 8dBi antennas, respectively. This highlights the potential benefits of using the directional antenna when it is properly selected. It also suggests a more directional antenna may not necessarily be better.

4.5 Predictability of RSS

By utilizing the RSSI traces collected in the previous chapter, we study how predictable the RSS from directional antennas is during real usage. We examine the zero order and first order prediction methods as discussed in Chapter 3.3. The prediction algorithms are performed on the very lightly smoothed RSSI traces, to reduce the effect of high frequency noise in RSSI readings. Figure 7 presents the prediction errors. Results show the median RSS prediction error is no more than 0.1dB for intervals of 10ms and 100ms. Similar to rotation prediction, our results show that RSS is very predictable in short intervals. Therefore, we will use this high accuracy of RSS predictions in designing our antenna selection algorithms, which will be discussed in Chapter 6 and Chapter 7.

Chapter 5 Multi-Antenna Design (MiDAS)

The characterizations presented in Chapter 3 and Chapter 4 suggest the feasibility and the potential benefits of using directional antennas on mobile devices. Based on the findings, we present a multi-antenna design (MiDAS) that can be immediately deployed to mobile devices with a single RF chain. Figure 8 illustrates the design. We next describe several design decisions and the rationale underneath them.

First, *the design requires only a single RF chain*. Therefore, at a given time, only one antenna can be used or assessed. This makes the design immediately deployable to power and cost-constrained mobile devices that only have a single RF chain, such as wireless handsets.

Second, *the design consists of one omni directional antenna and one or more directional antennas*. The omni directional antenna is included for not only standard-compliance but also as a “safety belt” when a good directional antenna is difficult to identify. At a given time, only one antenna is selected by the transceiver through an antenna switch. This eliminates much of the requirements on antenna spacing by MIMO and beamforming technologies, allowing MiDAS to fit in small form-factor devices.

Third, *the design considers the directional antennas only for data transmission and receiving their acknowledgments, which are used for antenna assessment*. It uses the omni directional antenna for other purposes, e.g., for idle listening, control packets, management packets, and data reception, or for data transmission in case a better directional antenna is not identified. The reasons for these design decisions are 1) A directional antenna improves the device energy efficiency much more in transmission

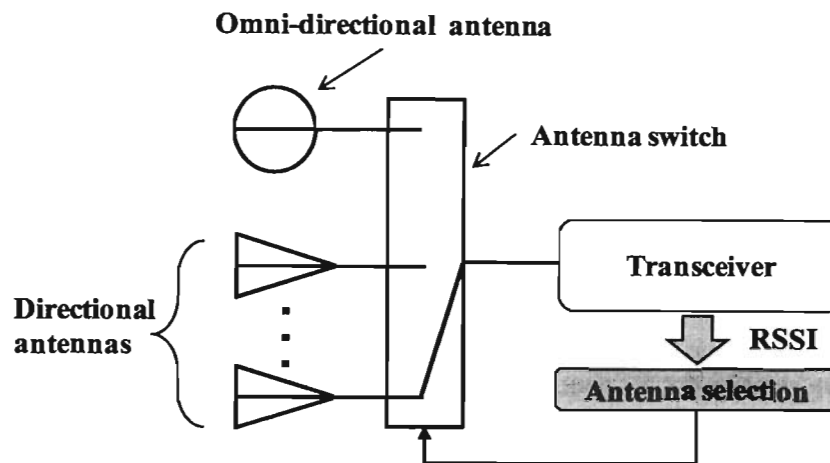


Figure 8: Multi-antenna system with one omni directional antenna and one or more directional antennas that works with existing wireless interfaces with a single transceiver

than reception; and 2) listening with directional antennas increases the deafness of the nodes. This is particularly important to CSMA-based 802.11 because the mobile client cannot accurately predict the arrival of incoming packets.

Key Research Question: With the multi-antenna system described above, the key question to be answered is: *which antenna to use for transmission?* In the next two chapters, we answer this question with two antenna selection methods. The first one assesses antennas by packets, and therefore does not require any changes to the deployed network infrastructure. The second one assesses antennas by physical layer symbols, which is much more efficient, but requires changes to the PHY layer.

Chapter 6 Selection for Legacy Networks

We first focus on mobile clients of legacy infrastructure networks such as deployed 802.11 and cellular networks. To work with legacy networks, the client must select the best antenna without any support from the infrastructure.

6.1 Packet-based Antenna Assessment

Without any changes to the deployed infrastructure, a mobile client can only assess one antenna per packet by measuring the average RSSI of certain bytes of the packet transmitted by that antenna and leveraging the channel reciprocity to estimate the receiver RSSI. Fortunately, as observed by us in Chapter 4.3 and by others [15], 802.11 channels often see good reciprocity.

To assess an antenna, the client transmits a packet and receives the ACK packet with the same antenna. To assess N antennas, the client has to accomplish N Data-ACK exchanges. In 802.11, each Data-ACK exchange can take several milliseconds, depending on the data rate and packet size. This ACK-based assessment comes with a cost in both network capacity and client efficiency. When an inferior antenna is being assessed, the Data-ACK exchange might be unsuccessful and therefore results in retransmission of the data packet. Such cost can potentially be reduced by sending empty packets and using their ACKs for antenna assessment.

6.2 Antenna Bookkeeping

Because finding the best antenna incurs cost and the superiority interval of the best antenna may be short, it is not always worthwhile to find out the best antenna. Therefore, we make some design decisions in the packet-based assessment discussed below. The goal of these decisions is to keep the client updated regarding its antennas in order to avoid unnecessary attempts to find out the best antenna. We call it *antenna bookkeeping*.

First, the client continuously assesses the antenna in use, either omni directional or directional. That is, the client always uses the same antenna to finish a Data-ACK exchange. This allows the client to detect changes in the channel of the antenna in use almost immediately.

Second, the client opportunistically assesses the omni antenna by using it for idle listening and data reception. Therefore, it can obtain the RSSI of the omni from the overheard packets sent by the infrastructure to its peers.

Finally, the client leverages the beacons broadcast by the access point, every 100ms by default in 802.11, to guarantee the omni antenna and some directional antennas are assessed frequently. When a directional antenna is used for data transmission and therefore continuously assessed, the client uses the beacons to guarantee the omni antenna is assessed every few hundred milliseconds. When the omni antenna is used for data transmission and therefore continuously assessed, the client uses the beacons to guarantee that directional antennas are assessed every few hundred milliseconds.

Using these three mechanisms, we can obtain the RSS of the antenna used for data transmission, and the RSS of the antennas used for receiving other packets (idle listening and beacons) as time series. We denote the time series of the RSS for an antenna as $S(t)$

where t is the time of assessment. Let t_n denote the time for the most recent assessment, t_{n-1} for the one before it and so on. We can calculate several important measures of the RSS for each of these antennas:

- Exponential moving average of RSS: $Savg(tn)$
- The rate of RSS change $R(tn)$:

$$R(tn)=[Savg(tn)-Savg(tn-1)]/(tn-tn-1)$$

- The first order prediction of RSS: $\hat{Savg}(tn+1)$

The exponential moving average is used mainly to smooth out the high frequency noise in RSSI readings for better RSS predictions, as discussed in Chapter 4.5

6.3 Heuristic Antenna Selection Algorithm

The key problem is to decide whether the client should assess the antennas to find out the best one or simply use the omni directional antenna. Our solution to this problem is based on two intuitive observations:

- First, if the client orientation and location have not yet changed much from last antenna assessment, the client should continue with the last identified best antenna.
- Second, if the channel is likely to change rapidly, it is better to use the omni directional antenna without assessing the antennas. The reason is that if the channel is likely to change a lot, the identified best antenna will not bring much benefit before its optimality expires. The tipping point of the change rate is actually dependent on the packet transmission rate: the higher the rate, the more benefit the best antenna can bring in before its optimality expires.

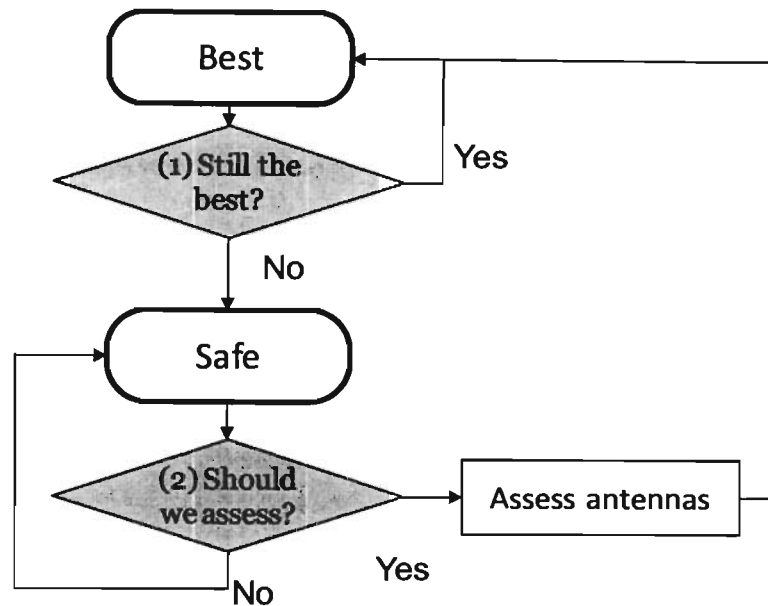


Figure 9: The packet-based antenna selection with two modes: Best and Safe. The client transits between the two modes according to two decisions

We leverage these two observations and devise a simple selection algorithm as illustrated by Figure 9. The algorithm has the client working in one of the two modes: *Best*, and *Safe*. In the *Best* mode, the client uses the antenna that was identified as the best antenna for data transmission from last antenna assessment. In the *Safe* mode, the client uses the omni antenna and does not know which antenna is the best. While the client may benefit from directional antennas in the *Best* mode, the *Safe* mode provides a “safety belt” that the client can resort to when the use of directional antennas is considered risky, especially when the client experiences frequent rotation or rapid mobility. The client transits between these two modes according to the answers to the following two questions:

- In the Best mode, is the last identified best antenna still the best? The client considers the current antenna no longer the best if the predicted RSSI of current antenna, \hat{S}_{avg} , is lower than that of any other antennas assessed in the last 100ms.
- In the Safe mode, should the client assess the antennas to identify the best one, or should it just keep on using omni? According to the second observation above, the client bases the decision on both the channel changes and the packet interval. Packet interval, T , is known to the client. The client gauges the channel change with the rate of RSS change, R , of the directional antenna that is assessed most recently. The client bases the decision on the product of $|R|$ and T . If their product is greater than a threshold, the client will remain in the Safe mode without assessing antennas. We experimentally choose 2dB for the threshold in the implementation, as it shows fast and cautious recovery from the Safe mode.

Chapter 7 Selection with PHY Support

We next show that antenna selection can be much more efficient and effective by assessing all antennas with PHY training symbols. Unlike the packet-based antenna selection, this PHY symbol-based method requires changes to the network infrastructure. Therefore, we target it for the long-term deployment of directional communication.

With PHY support, all the antennas are examined in a single packet. That is, a mobile client transmits a series of PHY training periods, each from one of the antennas so that the receiver can estimate the RSSI of all antennas and notify the mobile client of the best. This antenna selection strategy is one form of active probing of the transmit antennas.

7.1 PHY Symbol-based Antenna Assessment

The method is inspired by the 802.11 Physical Layer Convergence Protocol (PLCP), in particular the 802.11n MIMO PLCP. The 802.11 PLCP employs *training symbols*, for the receiver to estimate the channel and decode the packet. We employ training symbols similar to the 802.11n MIMO PLCP and existing antenna selection methods for MIMO, e.g., [16]. Each antenna takes turn to transmit the training period (8 μ s in 802.11). Knowing the number of training symbols per antenna, the receiver detects the symbols that belong to each antenna, and estimates the RSSI for that antenna. The receiver then notifies the transmitter of the antenna with the strongest channel. This feedback from the receiver to the transmitter makes the transmitter antenna selection different from and more challenging than antenna selection on the receiver side.

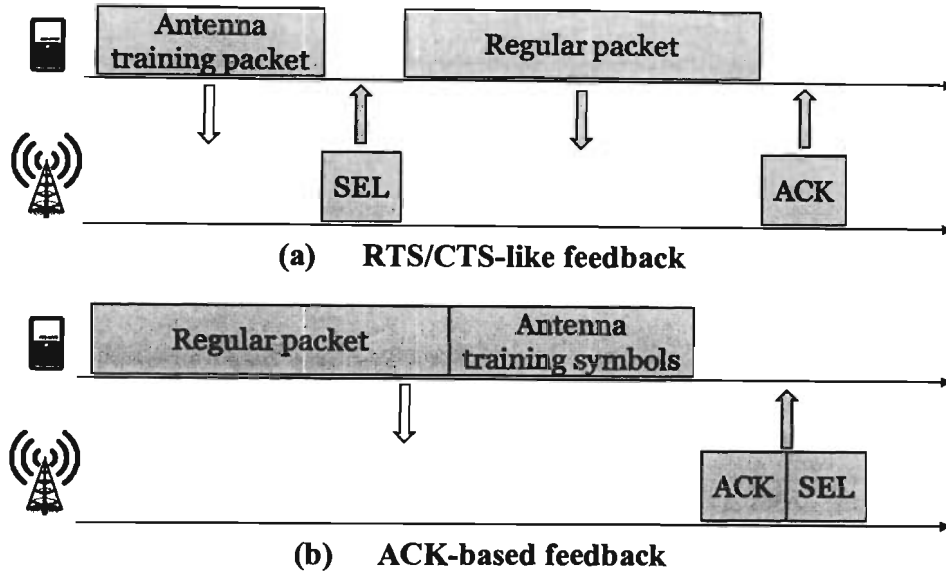


Figure 10: Two different ways for the receiver to notify the mobile client of the best antenna for symbol-based antenna selection

7.2 Selection Feedback

Because the transmitting mobile client does not need the RSSI values, the receiver can simply send back the index of the best antenna with $\log N$ bits, N being the number of antennas. There are two ways that the receiver can notify the transmitting mobile client, as illustrated in Figure 10. First, the receiver notifies with the ACK packet so that the transmitter can use the selected antenna for the next packet. We call this ACK-based feedback. The feedback will incur almost no overhead under 802.11. Second, the transmitter and receiver can use an exchange similar to RTS/CTS so the transmitter can use the best antenna for the current data packet. We call this RTS/CTS-like feedback.

The ACK-based feedback is only effective if the packet intervals are so short that the best antenna selected during one packet transmission will remain the best for the next. On the other hand, it is more efficient than the RTS/CTS-like feedback because the latter

incurs overhead due to the extra packet exchange. Therefore, MiDAS uses the ACK-based method only when the packet interval is short, below 100ms in our realization according to the characterization in Chapter 4. Otherwise, it employs the RTS/CTS-like feedback.

Chapter 8 Evaluation

We have implemented MiDAS with up to three directional antennas on the WARP platform. Using this implementation, we are able to collect traces for a detailed simulation study and also to perform real-time experiments to demonstrate the effectiveness of the packet-based and symbol-based antenna selection methods.

8.1 Hardware Implementation

A WARP node can accommodate up to four antennas using two radio cards. Each radio card has two antenna ports and can select from only two antennas in real time. Due to this limitation, we have to connect four antennas using two radio cards and select the antenna by first selecting the radio card and then selecting the right antenna. The unselected radio card is powered off. Therefore, there is only one radio card active at a time. While this implementation is less efficient than the switch-only realization as discussed in Chapter 5, it demonstrates the feasibility and gain of MiDAS and its antenna selection methods in real-time communication. The latency to switch between antennas is around 50ns, negligible in comparison to the PHY training period duration ($8\mu\text{s}$). Figure 11 (a) shows the physical placement of the three directional antennas and two different ways to use two of them only (*two-opp* and *two-adj*).

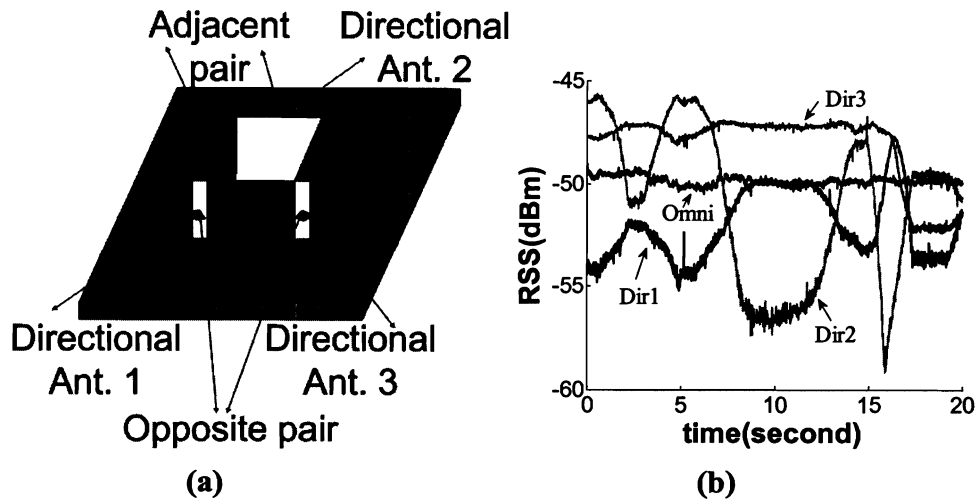


Figure 11: (a) Physical arrangement of the three directional antennas used in the trace collection and experimentation (b) A segment of RSSI trace for three 5dBi antennas in NLOS indoor environment

The antennas in the prototype are placed as close to each other as possible. This is because the antennas need to have highly correlated channels to achieve antenna pattern diversity, which is the goal of MiDAS. Considering that only one antenna is active at a time, there will be no constraint on the distance between antennas and they can be as close as possible. This means that not only placing the antennas close to each other on the sides of a small form factor smartphone is not constraint by the distance requirements known in MIMO and beamforming schemes, but also it is desirable.

We have implemented both packet-based and symbol-based antenna selection on the prototype. However, only the packet-based implementation is ready for real-time 802.11-like communication at this moment.

8.2 Trace Collection

To evaluate the antenna selection methods under controlled settings, we first collect RSSI traces of all four antennas of the hardware prototype. The RSSI traces are collected

using the same experimental setup with the motor platform replaying field-collected rotation traces as described in Chapters 4.1 and 4.4. There is one difference though. That is, four antennas, three directional and one omni directional, are used in the experiments. Therefore, the prototype repeatedly transmits a training period of 128 symbols from each of the four antennas in turn as fast as possible. The AP node measures and records the RSSI of all of the antennas. As a result, we are able to measure the RSSI of each antenna approximately every 10ms. We collect traces for three 5dBi and three 8dBi directional antennas, each in various propagation environments, including NLOS indoor, LOS indoor, and outdoor, as described in Chapter 4.1. The same transmit power of 18dBm is used for all experiments. Figure 11 (b) presents a segment of the RSSI traces of the four antennas for NLOS indoor.

8.3 Trace-based Simulation

The RSSI traces allow us to simulate the impact of various aspects of the antenna selection methods in a controlled manner. In the following, the simulation default assumes 1) the traffic is Poisson with the mean packet interval of 10ms; 2) the configuration of the multi-antenna system is three identical directional antennas and one omni directional antenna; 3) directional antennas have 5dBi peak gain; and 4) the environment is NLOS indoor. By changing each of these four aspects, we are able to reveal their impact on the system performance, reported in terms of RSS gain at the AP over that of the omni directional antenna case. That is, we report the difference between the RSS achieved by the proposed multi-antenna system and that by a traditional omni directional system. For each evaluation, we show the system performance for three

antenna selection methods: the genie-aided *upper bound* that knows the best antenna for every packet, the *packet-based* and *symbol-based* antenna selection methods according to Chapter 6 and Chapter 7, respectively. Figure 12 summarizes the results. Each bar in the graphs shows the median gain (in dB) of MiDAS antenna selection algorithms over an omni system in different scenarios. We also include the 10th and 90th percentile values of this gain in each bar. We make the following observations.

First, both symbol-based and packet-based antenna selection methods achieve very good gain (close to the upper bound) when traffic is intensive, i.e., average packet interval is below 100ms, as is apparent from Figure 12 (a). The packet-based method is slightly worse than the symbol-based because the packet-based method is much coarse-grained and has higher overhead in antenna assessment as discussed in Chapter 6 and Chapter 7. Moreover, neither of the two antenna selection methods ever falls below the omni directional antenna case and therefore the safety belt provided by the omni directional antenna does work. The packet-based method provides little gain when the traffic become sparser (packet interval \gg 100ms) while the symbol-based antenna selection method always achieves a performance close to the upper bound. Yet the symbol-based method achieves so with the cost of using the RTS/CTS-like selection feedback described in Chapter 7. The results show that for the traffic with average packet interval of 10ms, the RTS/CTS-like feedback is almost never used and therefore does not introduce any overhead. However, the percentage grows as the traffic becomes sparser, and we observe 36%, 90%, and 98% usage of RTS/CTS-like feedback for traffics with average intervals of 100ms, 1s, and 10s, respectively. Therefore, the multi-antenna system is more effective in more demanding networks that have more packets to transmit.

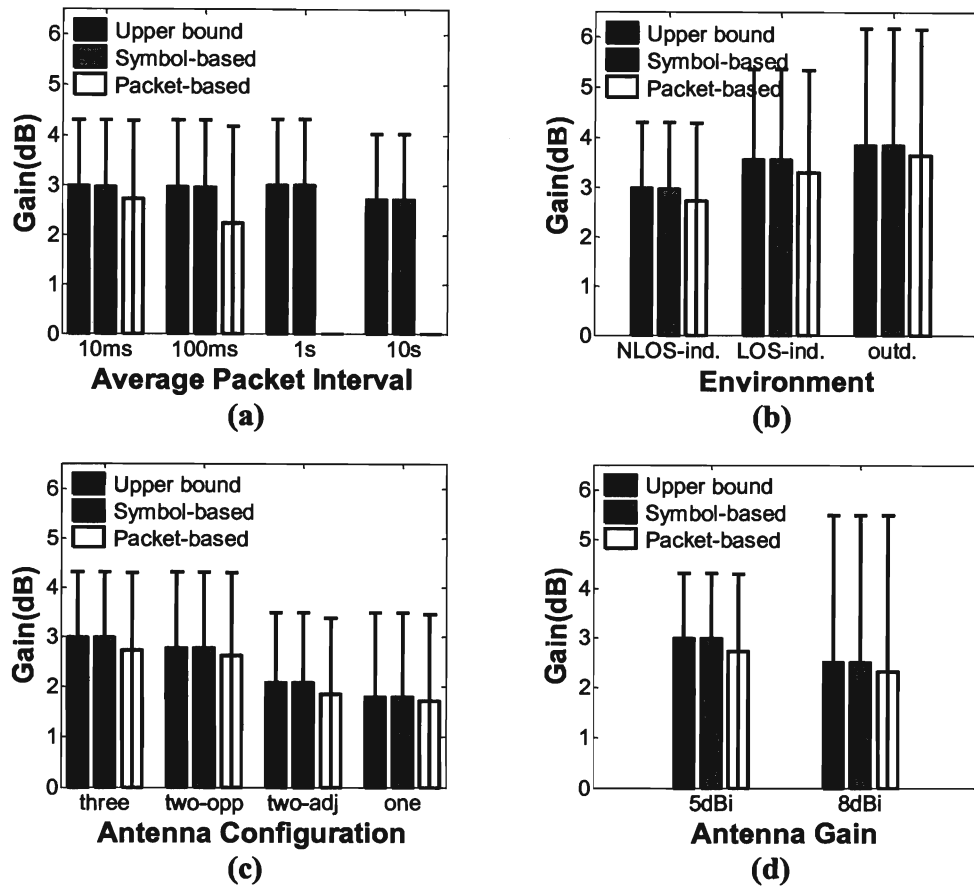


Figure 12: Impact of system settings on the performance of the multi-antenna system. Each bar presents the median, 10th and 90th percentile gain for three antenna selection cases: 1) *upper bound* assuming the best antenna is always used; 2) *symbol-based* antenna selection described in Chapter 7; and 3) *packet-based* antenna selection described in Chapter 6

Second, MiDAS and the two antenna selection methods work well for all propagation environments, as can be observed from Figure 12 (b). On the other hand, we observe that they provide more gain for LOS indoor and outdoor environments. This is not surprising as the same directionality usually leads to lower receiver gain under rich multi-path effects, as we have observed in Chapter 4 (Figure 5).

Third, our results indicate that a design with two directional antennas will provide much of the benefit of the directionality, as is apparent from Figure 12 (c). It also shows

that the opposite pair (*two-opp*) provides more gain than the adjacent pair (*two-adj*) as illustrated in Figure 11. Because *two-opp* covers a larger angular range than *two-adj*, we do expect that *two-opp* outperforms *two-adj* averagely, although it is possible that *two-adj* outperforms *two-opp* under certain propagation environments. Moreover, MiDAS provides decent gain even with only one directional antenna. Note that all these configurations also have one omni directional antenna in addition to their directional antennas.

Finally, our results indicate a more focused antenna may not necessarily provide higher gain. As observed from Figure 12 (d), MiDAS with three 5dBi antennas achieves better gain than that with three 8dBi antennas, even for the upper bound case. Comparing Figure 12 (c) and Figure 12 (d), we can see even two 5dBi antennas outperform three 8dBi antennas. Recall Figure 6 from Chapter 4. There we observed that the 5dBi antenna provides longer superiority intervals than the 8dBi one. As a result, MiDAS with 5dBi antennas requires less frequent antenna assessment and antenna changes.

8.4 Number of Directional Antennas:

Our trace-based simulation results showed that with three 5dBi directional antennas, MiDAS provides ~ 3 dB gain compared to a conventional omni system. But due to the hardware limitation in WARP, we were unable to investigate the performance of more than three directional antennas. Using the NLOS channel characterization of directional antennas in Figure 5, we try to answer the following question in this chapter: *How much will more directional antennas help?*

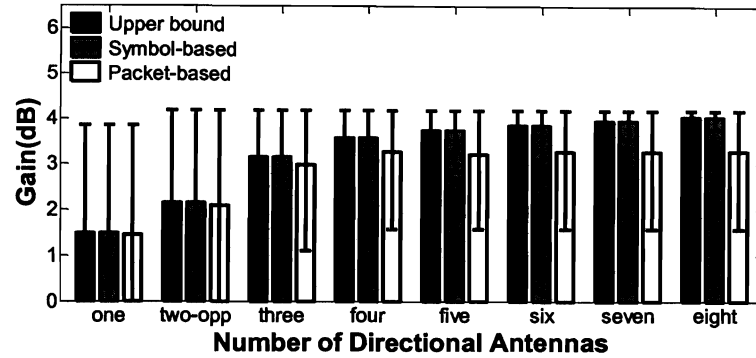


Figure 13: Impact of number of directional antennas on the performance of *upper bound*, MiDAS *symbol-based*, and MiDAS *packet-based*

We use the same one hour mobility trace that we used in our previous experiments along with the results in Figure 5 to emulate the performance of one to eight 5dBi directional antennas in NLOS indoor. All scenarios use a Poisson distribution with the average time interval of 10ms. Figure 13 shows the results for the genie-aided upper bound gain and the MiDAS antenna selection algorithms. We make three observations: First, the increase in the upper bound gain is marginal for more than 4 directional antennas. Second, MiDAS symbol-based always performs close to the upper bound. But it is important to note that more directional antennas introduce additional training overhead to MiDAS symbol-based, which increases linearly with the number of antennas. Third, as also observed in Figure 12 (c), the performance gap between the upper bound and the MiDAS packet-based increases as the number of antennas increases due to the additional assessment overhead, and as a result, the gain of MiDAS packet-based does not increase anymore for more than 4 directional antennas.

8.5 Moving Scenario

In all of the experiments reported above, the AP and client did not change locations while the client was rotating on the motor platform. In this chapter, we try to answer the following question: *What is the possible gain of MiDAS when the client moves?*

Instead of moving the client being rotated by the motor, we mount the AP on a cart and move the cart around at a walking speed until the connection is lost. During the mobility, the setup experiences both NLOS and LOS indoor environments. The average packet interval is set to be 10ms.

We observe that the upper bound gain, the symbol-based and packet-based antenna selections achieve average gains of 4.5dB, 4.4dB, and 2.6dB, respectively, compared to 3.0dB, 3.0dB, and 2.7dB, when the AP is not moving. Therefore, MiDAS maintains its gain even in moving scenarios. We believe that the reason for high upper bound gain of this scenario is that the antennas on the client, although mounted as close to each other as possible, are not fully correlated. Therefore, the system also benefits from spatial diversity at some spots.

Chapter 9 MiDAS with Rate Adaptation and Power Control

In this chapter, we apply rate adaption and transmit power control to MiDAS, MiDAS+RA/PC, to fully realize its gain in terms of goodput and power saving. Goodput is defined as the ratio of the delivered data payload to the transmission time. We show that MiDAS can increase the link goodput significantly in low SNR scenarios and reduce the transmit power noticeably in high SNR scenarios.

We adopt the SNR-triggered rate adaptation because it has been shown to outperform other mechanisms if trained well [17] and MiDAS already uses highly accurate link RSS prediction that can be translated to SNR predictions. SNR-triggered rate adaptation mechanisms use the goodput-SNR table, which maps the link SNR to its expected effective goodput for each physical layer data rate in the hardware. Deriving the goodput-SNR table is a one-time effort given a wireless interface card.

We apply rate adaptation and power control to MiDAS with packet-based antenna selection as follows. If MiDAS is in the Best mode, for every packet, MiDAS predicts the link SNR using the methods discussed before. Then it uses the goodput-SNR table and chooses the rate that has the highest expected goodput in the predicted link SNR. Using the goodput-SNR table, MiDAS also reduces its transmit power as much as the expected goodput is not reduced by more than a defined percentage e.g., 1%, also known as the *goodput loss threshold*. The threshold can be chosen to be 0% if the device is unwilling to sacrifice any goodput. If MiDAS is not in the Best mode, we choose the base rate and no power control is applied, in order to maintain the “safety belt”. Algorithm 1 presents a detailed description of the algorithm used in MiDAS+RA/PC for packet-based antenna

Algorithm 1: Rate adaptation and power control in MiDAS with packet-based antenna selection

Input: Predicted SNR value for the next packet (\hat{s}) in dBm, the goodput-SNR table

($G_r(s)$) for all possible rates ($r = 1, 2, \dots$), goodput loss threshold (l)

Output: optimal rate (R), and maximum transmit power reduction (P) in dB

```

1  If in best mode
2  pick  $R = \operatorname{argmax}_r G_r(\hat{s})$ 
3  pick  $P = \max_p p$  s.t.  $G_R(\hat{s} - p) \geq (1 - l) \cdot G_R(\hat{s})$ 
4  else
5  pick the base rate ( $R = 1$ )
6  pick  $P = 0$ 
7  end

```

selection. The same algorithm can also be applied to MiDAS with symbol-based antenna selection.

9.1 Simulation Results

We simulate MiDAS+RA/PC with the channel traces. Our simulation uses the rates supported by 802.11a. We use the effective goodput-SNR table reported by the authors of [18] for eight 802.11a rates using 2000 byte packets. The goodput loss threshold is chosen to be 1%.

Figure 14 shows the results. We observed that the performances of packet-based antenna selection and symbol-based antenna selection are very close to each other in terms of goodput gain and power saving. Therefore, we only show the results for packet-

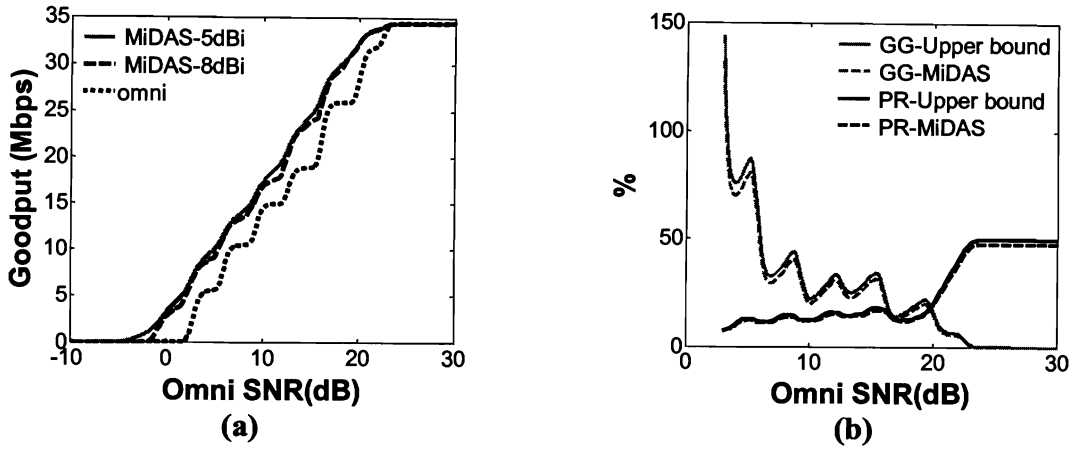


Figure 14: (a) Goodput of MiDAS+RA/PC (three 5dBi and three 8dBi) and Omni+RA in NLOS indoor; (b) Goodput Gain (GG) and transmit Power Reduction (PR) of MiDAS+RA/PC (three 5dBi) versus omni+RA in NLOS indoor

based antenna selection, which has a slightly worse performance than symbol-based antenna selection. Also the baseline for the performance comparison is an omni system that also uses the same rate adaptation algorithm. We have not included power control in the baseline omni algorithm because the effect of omni transmit power is already included in the corresponding omni link SNR in the x axis of both graphs in Figure 14.

Figure 14 (a) shows the goodput of MiDAS+RA/PC with three 5dBi and three 8dBi antennas. The same figure also shows the goodput for the baseline omni+RA system. We make the following observations: First, three 5dBi antennas outperform three 8dBi antennas. Second, there are some SNR values for which omni system has no connection or its goodput is low (below 3.3 Mbps), but MiDAS+RA/PC is capable of maintaining a much higher goodput. We refer to these SNR values as “Weak or no connection” region. Third, MiDAS+RA/PC always outperforms the omni system. Figure 14 (b) shows the performance of MiDAS+RA/PC in terms of goodput improvement and power reduction for three 5dBi antenna compared to the omni system. We have not plotted these graphs

for “Weak or no connection” region, because the goodput gain can be infinite in this regime. The first point in Figure 14 (b) corresponds to the SNR value in which omni system has 3.3Mbps goodput.

We have also computed the genie-aided upper bound for the two evaluated metrics with the assumption that the node has perfect knowledge of channel conditions in the future. The results show that MiDAS+RA/PC has a performance very close to the upper bound. The results show that, for omni-SNR = 3 dB, where omni system has a goodput of 3.3Mbps, MiDAS+RA/PC increases the goodput by 132% while reducing the transmit power by 7%. Also, for omni-SNR = 30 dB, where omni system has a goodput of 34.4 Mbps, MiDAS+RA/PC maintains the same goodput while reducing the transmit power by 48%

9.2 Real-Time Experiment Results

We implemented MiDAS+RA/PC in WARP for real-time experimentation. The WARP current physical layer only supports three different modulations, being BPSK, QPSK, and QAM16 which correspond to 6, 12, 24 Mbps physical layer rates. The physical layer in WARP is uncoded; hence supported rates differ in their modulations only. We choose to implement an SNR-triggered rate adaptation with equal air time to benefit more from higher data rates. That is, the data size of the packet is bigger for higher rates in order to have equal transmission periods over the air for all rates.

First, we derive the goodput-SNR table for different rates in WARP with equal air time packets. To do so, we connect two WARP boards over wire with 60 dB attenuation in between. The choice of wire is to emulate a constant SNR medium. Therefore, the

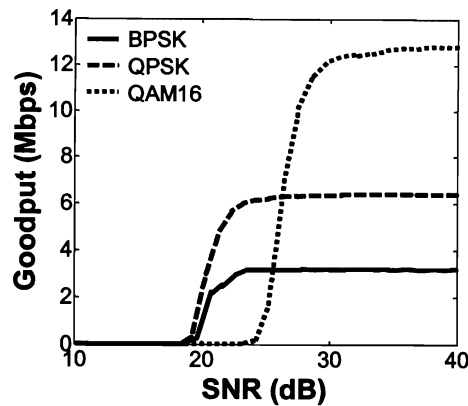


Figure 15: Effective goodput of different modulations in WARP with equal-air-time packets.

goodput values in this table are the expected value of goodput given some predicted SNR. In our experiment, we change the transmit power over all possible values. For each transmit power, we send packets as fast as possible for 30 seconds. The size of the data part of the packet is 1400 bytes for QAM16 modulation, and is modified accordingly for other modulations to have equal air-time. Figure 15 shows the results. We observe that QPSK modulation always outperforms BPSK over all possible SNR values in terms of link goodput. Therefore, an SNR-triggered rate adaptation algorithm will not choose BPSK at any input SNR. This means that we can only benefit from the other two modulations in our experiments.

We performed two experiments using three 5dBi directional antennas. The client is placed on the motor platform which rotates according to the traces, and the AP is stationary, and each experiment lasts for 20 minutes. The packets are transmitted as fast as possible using the selected modulations. In the first experiment, the omni antenna experiences a low SNR which is not enough to use the QAM16 modulation. In the second experiment, the omni link is strong enough to switch to the higher modulation. The

results show that, in the first experiment, the gain from MiDAS is enough to switch to the higher modulation for most of the packets, and therefore the goodput is increased by 85%, using the same transmit power as the omni transmitter. In the second experiment, this gain from MiDAS is used to save transmit power by 51% while increasing the goodput by 7%.

Chapter 10 MiDAS with Rate Adaptation and Power Control

We next discuss related work in smartphone orientation estimation, directional communication, directional antenna, and antenna diversity. In summary, all existing work considers smartphone-like mobile devices as omni directional.

Smartphone Orientation Estimation: Accelerometers and compasses have been used for different purposes. These applications include localization [19], inferring the orientation of the device in motion [20], and monitoring the road and traffic conditions in a city [21], which includes estimating the tilt angles of the phone (θ , φ). However, no previous work has characterized the rotational patterns of real-life usage of smartphones, and to the best of our knowledge, our work is the first to do so.

Directionality based on Smart Antenna System: Beamforming using smart antenna systems has been widely studied and deployed for cellular base stations (e.g., [22]), WLAN access points (e.g., [2]), and even vehicles (e.g., [23]), but not for battery-powered mobile devices like smartphones. Compared with MiDAS, beamforming requires multiple RF chains and therefore comes with much higher power and hardware cost. Therefore, compared to beamforming based directional communication, MiDAS is more amenable to immediate deployments due to its small changes to the hardware and infrastructure.

Directionality from Directional Antenna: Directional antennas have also been studied for 802.11 mesh nodes (e.g., [8]) and sensor nodes (e.g., [24]). Because existing work only applies directional antennas to fixed platforms that do not move or rotate, it does not address the antenna selection challenge that must be solved for use on mobile devices.

Our previous work, BeamSwitch [25], is the most related work. It requires the directional antennas to be placed in a way to form an omni directional coverage. It employs some form of packet-based antenna assessment to identify the best directional antenna all the time. In contrast, we do not have any constraints on the number or placement of antennas. Moreover, we show that it is not always worthwhile to find out the best antenna and therefore answer a different question: *should the antennas be assessed or not?* Also, we study the much more efficient symbol-based antenna selection method so that the order of antenna assessment is no longer important.

Antenna Diversity on Mobile Devices: Mobile devices such as wireless handsets have used multiple (often two) omni-directional antennas for *antenna diversity*, e.g., see [26, 27]. Compared to MiDAS that uses directional antennas, antenna pattern diversity from omni directional antennas is lower, and the benefit is mainly due to spatial diversity. Some mobile devices actually use two directional antennas to form an omni directional antenna and treat them as a single antenna for communication. Therefore, they do not gain from the directionality of the directional antennas. Also, all the antenna selection algorithms for receiver diversity systems are intended for the receiver side, which makes them different from MiDAS.

Chapter 11 Conclusions

We make the following conclusions following the characterization, simulation, and experimentation reported in this work.

- Through MiDAS and its antenna selection methods, directional antennas can be effectively employed to improve the transmission gain of smartphone-like mobile devices by almost 3dB under various propagation environments and realistic rotation. Such gain can be achieved without any change to the deployed network infrastructure.
- Three 5dBi antennas, placed on the adjacent sides of a mobile device, can provide 3dB gain of MiDAS.

Such gain is possible because of the following characteristics we identified from field-collected traces and trace-driven experimentation with directional antennas:

- Smartphone-like devices rotate relatively slow, below $120^\circ/\text{second}$ for 90% of the time for each Euler angle, during wireless usage, compared to how fast modern wireless clients exchange packets with their access point or base stations.
- The channel of directional antennas is quite reciprocal at least under various 802.11 propagation environments.
- The channel of directional antennas is quite predictable in short terms (100ms or shorter) when the device is undergoing human-inflicted rotations.

- Directional antennas with a higher gain may not necessarily be better because they will be good for a shorter period of time under device mobility and rotation, in comparison to ones with a lower gain.

Finally, by experimentally demonstrating the link gain of passive directional antennas on mobile devices, this work is an important step toward an efficient network of directional mobile clients. It invites further research into many interesting networking problems when mobile clients employ directional communication solutions like MiDAS.

References

- [1] M. Blanco, R. Kokku, K. Ramachandran, S. Rangarajan, and K. Sundaresan, "On the Effectiveness of Switched Beam Antennas in Indoor Environments," in *Proc. Passive and Active Measurement (PAM)*, April 2008.
- [2] X. Liu, A. Sheth, M. Kaminsky, K. Papagiannaki, S. Seshan, and P. Steenkiste, "DIRC: Increasing Indoor Wireless Capacity Using Directional Antennas," in *Proc. ACM SIGCOMM*, August 2009.
- [3] R. R. Choudhury, X. Yang, R. Ramanathan, and N. H. Vaidya, "Using Directional Antennas for Medium Access Control in Ad Hoc Networks," in *Proc. ACM MobiCom*, September 2002.
- [4] A. Amiri Sani, L. Zhong, and A. Sabharwal, "Directional Antenna Diversity for Mobile Devices: Characterizations and Solutions," in *Proc. ACM MobiCom*, September 2010.
- [5] Telex, *5dBi Patch Antenna*:
<http://www.telex.com/Wireless/product.aspx?MarketID=1&CategoryID=3&ProductID=49>, 2008.
- [6] B. Cetiner, H. Jafarkhani, J. Qian, H. Yoo, A. Grau, and F. De Flaviis, "Multifunctional Reconfigurable MEMS Integrated Antennas for Adaptive MIMO Systems," in *IEEE Communications Magazine*, vol. 42, issue 12, 2004.
- [7] S. Zhang, G. Huff, J. Feng, and J. Bernhard, "A Pattern Reconfigurable Microstrip Parasitic Array," in *IEEE Transactions on Antennas and Propagation*, vol. 52, issue 10, 2004.

- [8] A. P. Subramanian, H. Lundgren, and T. Salonidis, "Experimental Characterization of Sectorized Antennas in Dense 802.11 Wireless Mesh Networks," in *Proc. ACM MobiHoc*, May 2009.
- [9] CRAWDAD, *User Study Traces*: <http://crawdad.org/rice/midas>.
- [10] H. Goldstein, C. P. Poole, and J. L. Safko, *Classical Mechanics*, 2nd ed.: Addison-Wesley, 1980.
- [11] Kionix, *Application Note: screen rotation and device orientation*: http://www.kionix.com/App-Notes/AN011_Screen_Rotation.pdf.
- [12] Maxim Integrated Products, *Datasheet for MAX2828-MAX2829, Single-/Dual-Band 802.11a/b/g World-Band Transceiver ICs*, 2008.
- [13] L-COM Global Connectivity, *RE08P: HyperGain 2.4 GHz 8 dBi Round Patch Antenna*: http://www.l-com.com/multimedia/datasheets/DS_RE08P-RTP.PDF.
- [14] Telex, *Omni-directional 2406 Antenna*: <http://www.telex.com/Wireless/Product.aspx?MarketID=1&CategoryID=3&ProductID=21>, 2008.
- [15] G. Judd, X. Wang, and P. Steenkiste, "Efficient Channel-Aware Rate Adaptation in Dynamic Environments," in *Proc. ACM MobiSys*, June 2008.
- [16] T. Onizawa, A. Ohta, and Y. Asai, "Experiments on FPGA-Implemented Eigenbeam MIMO-OFDM With Transmit Antenna Selection," in *IEEE Transactions on Vehicular Technology*, vol. 58, issue 3, 2009.
- [17] J. Camp and E. Knightly, "Modulation Rate Adaptation in Urban and Vehicular Environments: Cross-Layer Implementation and Experimental Evaluation," in *Proc. ACM MobiCom*, September 2008.

- [18] D. Qiao, S. Choi, and K. Shin, "Goodput Analysis and Link Adaptation for IEEE 802.11a Wireless LANs," in *IEEE Transactions on Mobile Computing*, vol. 1, issue 4, 2002.
- [19] M. Youssef, M. Yosef, and M. El-Derini, "GAC: Energy-Efficient Hybrid GPS-Accelerometer-Compass GSM Localization," in *Arxiv preprint arXiv:1004.3174*.
- [20] K. Kunze, P. Lukowicz, K. Partridge, and B. Begole, "Which Way Am I Facing: Inferring Horizontal Device Orientation from an Accelerometer Signal," in *Proc. IEEE Int. Symp. on Wearable Computers (ISWC)*, September 2009.
- [21] P. Mohan, V. Padmanabhan, and R. Ramjee, "Nericell: Rich Monitoring of Road and Traffic Conditions Using Mobile Smartphones," in *Proc. ACM SenSys*, November 2008.
- [22] J. C. Liberti and T. S. Rappaport, *Smart Antennas for Wireless Communications: IS-95 and Third Generation CDMA Applications*: Prentice Hall PTR Upper Saddle River, 1999.
- [23] V. Navda, A. P. Subramanian, K. Dhanasekaran, A. Timm-Giel, and S. Das, "MobiSteer: Using Steerable Beam Directional Antenna for Vehicular Network Access," in *Proc. ACM MobiSys*, June 2007.
- [24] C.-L. Yang and W. J. Chappell, "Angular Diversity – Prominent for Compact Devices of Wireless Sensor Network in Indoor Environments," in *Proc. IEEE Antennas and Propagation Society Int. Symp. (APS)*, June 2007.
- [25] A. Amiri Sani, H. Dumanli, L. Zhong, and A. Sabharwal, "Power-Efficient Directional Wireless Communication on Small Form-Factor Mobile Devices," in

Proc. ACM/IEEE Int. Symp. Low Power Electronics and Design (ISLPED),
August 2010.

- [26] O. Norklit, P. D. Teal, and R. G. Vaughan, "Measurement and Evaluation of Multi-Antenna Handsets in Indoor Mobile Communication," in *IEEE Transactions on Antennas and Propagation*, vol. 49, issue 3, 2001.
- [27] J. S. Colburn, Y. Rahmat-Samii, M. A. Jensen, and G. J. Pottie, "Evaluation of Personal Communications Dual-Antenna Handset Diversity Performance," in *IEEE Transactions on Vehicular Technology*, vol. 47, issue 3, 1998.
- [28] M. Rogers, K. Hrovat, K. McPherson, M. Moskowitz, and T. Reckart, "Accelerometer Data Analysis and Presentation Techniques," Technical Report, National Aeronautics and Space Administration, Lewis Research Center, 1997.

Appendix A Trace Collection

We employ a commercial smartphone with a built-in tri-axis accelerometer and compass, HTC G1, to collect data regarding device orientation from real mobile device usage. We have developed a software logger to collect accelerometer and compass readings along with information regarding wireless network status, and applications being used for HTC G1. The logger runs in the background and collects data about every 10ms, including both voice and Internet usage. We employ a larger battery and an extended battery compartment cover for the HTC G1 so that the smartphone has 10 to 15 hours of battery lifetime with normal usage, long enough not to significantly affect participants' usage.

We recruited 11 participants through flyers distributed on Rice university campus to use the HTC G1 with their own SIM cards inside. We collected data from each for one week. Each participant was rewarded with a \$50 gift card. The collected data are available through CRAWDAD [9].

Appendix B Euler Angle Estimation

We next provide details regarding how we estimate the three Euler angles from accelerometer and compass readings.

B.1. Deriving Euler Angles

We assume that accelerometer only measures the gravity and compass only measures the electromagnetic field of the magnetic north. Moreover, we assume that sensor readings are error-free. In next chapter, we will explain the sources of inaccuracy in sensor readings and how to overcome them.

We use ax , ay , and az to show the three accelerometer readings for X , Y , and Z axes of the device (Figure 1). Similarly, we use cx , cy , and cz to show the three compass readings for the mentioned axes. All the other notations used in this chapter follow Figure 1.

We compute θ using accelerometer readings. θ is the angle between X and z , and it is straightforward to show that $\theta = \text{Arctan}(ax / \sqrt{ay^2 + az^2})$ [11].

We compute φ using accelerometer readings as well. φ is the angle between Y and the line of nodes, or N . N is equal to $\cos(\varphi)Y - \sin(\varphi)Z$, and is perpendicular to z . Therefore, it is straightforward to show that $\varphi = \text{Arctan}(ay / az) + 180 \cdot I_1(\cos(\varphi))$, where $I_1(x)$ is equal to 1 whenever x is negative, and is equal to 0 otherwise. The term $180 \cdot I_1(\cos(\varphi))$ is used to expand the 180 degree range of $\text{Arctan}(\cdot)$ to 360 degree range of φ . Moreover, $I_1(\cos(\varphi)) = I_1(az)$, and therefore $\varphi = \text{Arctan}(ay / az) + 180 \cdot I_1(az)$.

The previous equation outputs infinity when az goes to zero. This problem is the result of the Gimbal Lock problem [10], which happens when Y - Z and x - y planes coincide and

become indistinguishable. In this case, ψ and ϕ will be in the same plane and the Euler angle coordinates loses one degree of its freedom. Therefore, the orientation of the device can be described using θ and $\phi+\psi$ [10]. To overcome the Gimbal Lock problem in estimating ϕ , it is enough to set $\phi = 0$ when ay is zero, irrespective of the value of az . Therefore, we add a small offset to the dominator inside $Arctan(\cdot)$ to prevent it from being 0. That is $\phi = Arctan(ay / (az+0.1 \cdot I_2(az))) + 180 \cdot I_1(az)$, where $I_2(x)$ is equal to 1 whenever x is zero or positive, and is equal to 0 otherwise.. This new equation will assign 0 to ϕ during the Lock, while maintaining its smoothness. Also, because the small value of the offset, it will produce a close output in other cases than the Lock.

Finally we compute ψ using compass readings and the previously computed θ and ϕ . ψ is the angle between x and P , which is the reflection of X on x - y plane. x is in the P - N plane, and therefore $x = -\sin(\psi)N + \cos(\psi)P$. Moreover, x is perpendicular to y , and therefore $\tan(\psi) = P \cdot y / N \cdot y$. It is then straightforward to show that $\psi = Arccot((\cos(\phi) cy - \sin(\phi) cz) / \sec(\theta) cx) + 180 \cdot I_1(\sin(\psi))$. The term $180 \cdot I_1(\sin(\psi))$ is used to expand the 180 degree range of $Arccot(\cdot)$ to 360 degree range of ψ . Moreover, $I_1(\sin(\psi)) = I_1(cx)$, and therefore $\psi = Arccot((\cos(\phi) cy - \sin(\phi) cz) / \sec(\theta) cx) + 180I_1(cx)$.

B.2. Overcoming Hardware Limitation

In practice, there are a few challenges to the estimation algorithm from the hardware limitations of accelerometer and compass in smartphones. First, both the accelerometer and the compass are prone to hardware noise. In particular, the compass can be easily interfered by electromagnetic activities nearby, including those by the host device. From controlled measurement conducted in the lab, we observe that such interferences and

hardware noise tend to be much higher frequency than what could be possibly introduced by device rotation or mobility. Therefore, we suppress the noise and interference with a moving average window of 25 samples. Moreover, the numerical readings of a sensor can be different from the physical value. For example, when there is no acceleration, the accelerometer reading can be non-zero. We remove this offset by data demeaning [28]. Finally, while we leverage the impact of gravity on the accelerometer reading to estimate the orientation, the accelerometer reading also reflects the mobility of a device through acceleration. We note that the gravity is almost constant while the external acceleration due to mobility changes much faster. Therefore, the impact from mobility is suppressed with the mentioned low pass filter.

B.3. Validation of Orientation Estimation

We validate our orientation estimation algorithm with two experiments. In the first experiment (*static*), we place the HTC G1 smartphone on a plastic supporter in a series of orientations that are measured accurately as the ground truth. In the second experiment (*accelerated*), we fix the orientation of the phone and hand-move the phone with high acceleration toward various directions. In both experiments, we use our algorithm to calculate the orientation and compare it with the ground truth.

Table 1: Orientation estimation error (°)

Euler Angle	Static		Accelerated	
	Average	Maximum	Average	Maximum
θ	0.9	1.5	1.1	1.8
φ	3.8	9.5	1.5	3.3
ψ	11.7	21.1	4.6	9.5

Table 1 provides the average and maximum error for each of the Euler angles for both the experiments. As the results show, the estimation of θ is the most accurate. The estimation of φ has very small error in most of its range except for when θ is equal to 90 or -90 degrees, which is known as the Gimbal Lock [10]. ψ is the most error-prone angle. This is mainly due to the noisy compass reading. However, our interest is in the device rotation, instead of orientation. Because the random nature of the errors, we can consider the rotation derived from the orientation estimation acceptable for our characterization purpose.